Alexandria Engineering Journal (2020) 59, 177–189

HOSTED BY

ELSEVIER

Alexandria University

Alexandria Engineering Journal

www.elsevier.com/locate/aej
www.sciencedirect.com

ORIGINAL ARTICLE

Unsteady EMHD dual stratified flow of nanofluid with slips impacts

Yahaya Shagaiya Daniel [a,b,c], **Zainal Abdul Aziz** [a,b,*], **Zuhaila Ismail** [a], **Arifah Bahar** [a,b]

[a] *Department of Mathematical Sciences, Faculty of Science, Universiti Teknologi Malaysia, 81310 UTM Johor Bahru, Johor, Malaysia*
[b] *UTM Centre for Industrial and Applied Mathematics (UTM-CIAM), Ibnu Sina Institute for Scientific and Industrial Research (ISI-SIR) Universiti Teknologi Malaysia, 81310 UTM Johor Bahru, Johor, Malaysia*
[c] *Department of Mathematical Sciences, Faculty of Science, Kaduna State University, Tafawa Belewa Way, P.M.B 2339 Kaduna State, Nigeria*

Received 16 August 2019; revised 10 November 2019; accepted 3 December 2019
Available online 19 December 2019

KEYWORDS

Mixed convection;
EMHD nanofluid;
Thermal radiation;
Double stratification;
Slip flow

Abstract The present study explores the two-dimensional linear permeable stretched flow of nanofluid in the presence of double stratification and slip impacts. The mathematical model is developed in the presence of Joule heating, viscous dissipation and chemical reaction impacts. Nanofluid is electrically conducting in the presence of applied electric and magnetic fields. Suitable transformations yield the couple of nonlinear set of ordinary differential systems. The resulting system of equations has been solved numerically via implicit finite difference scheme. Graphs are plotted to examine the effects of physical emerging parameters on the velocity, temperature and concentration profiles. Also, the skin friction coefficients, local Nusselt and Sherwood numbers are computed and analyzed.

1. Introduction

Nanofluid involves dilute mechanical suspensions of ultrafine particles in an ordinary fluid, which significantly contributes to the intensification of thermal conductivity [1]. Due to the poor nature of heat transfer characteristics associated with the ordinary fluids, is the major challenge face for efficiency and high compactness in engineering applications through different models [2–8]. Furthermore, nanofluids are liquids with enriched thermal physical appearance which is widely applied to increase the strength of thermal energy in a system [9]. The fact is that fluid particles having thermal conductivities function higher and better as compared to ordinary fluids. Reinforced thermal energy is needed, where the Lorentz force decreases the convection flow within the system.

* Corresponding author at: Department of Mathematical Sciences, Faculty of Science, Universiti Teknologi Malaysia, 81310 UTM Johor Bahru, Johor, Malaysia.
E-mail addresses: shagaiya@kasu.edu.ng (Y.S. Daniel), zainalaz@utm.my (Z.A. Aziz), zuhaila@utm.my (Z. Ismail), arifah@utm.my (A. Bahar).
Peer review under responsibility of Faculty of Engineering, Alexandria University.

https://doi.org/10.1016/j.aej.2019.12.020
1110-0168 © 2019 Faculty of Engineering, Alexandria University. Production and hosting by Elsevier B.V.

Nomenclature

a	constant
b	stretching sheet constant
B_0	magnetic field factor
c_f	coefficient of Skin friction
D_B	coefficient of Brownian diffusion
D_T	coefficient of Thermophoresis diffusion
E_0	electric field influence
Ec	Eckert number
f_η	dimensionless velocity
J	Joule current
k	thermal conductivity
L_1, L_2, L_3	slips parameters
M	magnetic field
Rd	radiation constant
Nb	brownian motion number
Nt	thermophoresis number
Nu	local Nusselt number
Pr	Prandtl number
Re	local Reynolds number
s	suction/injection parameter
Sc	Schmidt number
Sh	local Sherwood number
s_m	mass stratification parameter
s_t	thermal stratification parameter
t	time
T	temperature of the fluid
T_W	variable wall temperature
T_∞	temperature at infinity
u, v	velocity constituent lengthways $x-$plus $y-$direction
v_W	wall mass transfer
V	fluid velocity

Greek symbols

α	thermal diffusivity
σ	electrical conductivity
$\sigma*$	Steffan-Boltzmann constant
η	variable of dimensionless-similarity
μ	fluid dynamic-viscosity
υ	fluid Kinematic-viscosity
$(\rho)_f$	nanofluid Density
$(\rho c)_f$	nanofluid-Heat-capacity
$(\rho c)_p$	nanoparticles-heat-capacity
ψ	stream function
σ	electrical conductivity
φ_W	surface nanoparticle concentration
φ_∞	infinity nanoparticle concentration
θ	dimensionless temperature
ϕ	dimensionless concentration
τ	nanofluid heat capacity to the nanoparticle heat capacity
λ	diffusion constant parameter
γ	chemical reaction

Subscripts

∞	condition at the free stream
W	condition at the surface

The deferral of magnetic nanoparticles in liquid tends to increase performance, and therefore strengthening the processing through the heat transfer. Consequently, the investigation associates to Lorentz force effects draws the attention of experts in the areas of engineering, and sciences, and these can be attributed to broadly industrial applications mostly in magnetohydrodynamic generators, the pumps, the bearings etc. see [10–12]. However, improvements in the field of nanoscience are initiated distinctly by exploring the materialistic characteristics of matter at the nanoscale level. Considering different applications of nanosciences, nanofluids institute new area over heat transfer see [13–15]. Mostly, fascinating research over the heat transfer focuses owing to its inclusive of scientific and engineering processing notice in polymer processing, microchips upscale computer-processors, hydrodynamical machines, micro-mechanical, chemical processing, hybrid-powered engines, food processing, nuclear engineering, cooling towers, air-conditioners/refrigerators, space cooling, and lubrication system [16–20]. Nevertheless, investigations analyzed on MHD mixed convection flow of conventional heat transfer fluids were performed in diverse fields using several geometries in [21–28]. Furthermore, nanofluids have attracted enormous interest particularly relating to their extraordinary thermal transport as well as its scientific and engineering applications.

Stratification surfaces in a liquid when the temperature fluctuations or distinctions in concentration, otherwise the occurrence of different liquids with varying densities, tends to form layering. Consequently, in water systems such as the rivers, lakes or pond, oceans, and reservoirs, salinity stratification in estuaries, change in temperature, distinct fathomage, and change in fluid's density and temperature refers to as stratification [29]. It is exceptional secure temperature [30], resonating body of water connected to certainly areas in a system. Sudden inclination away from fluid directed toward embodiment flow overlay, act unsettled extremely not high temperatures. Sudden degrees descents lower than the freezing point, as the coldest layer, flows change and rises up to the topmost of the layer. Nevertheless, in heat and mass transfer processes, simultaneous occurrence takes place. Considering double stratification (thermal and concentration [31]) due to convective flow in the fluid, arises in a different situation. It is frequently faced in power collectors, annealing and thinning of copper wires, reservoir mixing, liquid film, internal waves, condensation mechanisms of boundary layer, shear flow instability, desalination, internal hydraulics, solar human transpiration, crops damage originated from freezing, air conditioning, refrigeration etc. [32]. The fluids transpire with respect through degrees differences known as thermal stratification [33], not to mention the concentration variations also tagged as solutal stratification or even existence of diverse liquids attributed to varying densities, in a suspenseful system.

Advanced energy efficiency, enhances the system performance which is obtainable through well-defined stratification. It has numerous relevance's in physical phenomenon regarding with aerodynamic extrusion of sheets, geophysics, heat exchangers, metallurgy processes, and engineering fields just to mention the chemical engineering, petroleum engineering, ceramic (composite) engineering, and biochemical engineering [34]. However, presence of Lorentz force towards convective heat transfer in stratified fluid with engineering and industrial significance, is extremely crucial in heat and mass transfer fields. Two phase models using Buongiorno mathematical model was used by different researchers such as: Reported on MHD flow involving second-grade nanofluid induced by a nonlinear stretching surface with deforming thickness was given by Hayat et al. [35]. Analysis of double stratifications in magneto-nanomaterials by nonlinear stretching sheet is addressed by Hayat et al. [36]. Also, the aspects of Joule dissipation, heat generation and thermal radiation are considered by Waqas et al. [37] that analyze the heat transportation analysis. The research work on doubly stratified medium subject to both magnetized and non-magnetized flow fields was discussed by Rehman et al. [38].

The objective of this investigation is to study the flow of unsteady electromagnetohydrodynamic (EMHD) nanofluid in the presence of double stratification with slips conditions over a vertical stretching using Buongiorno mathematical model [39]. The application is to reduce the skin friction coefficient and enhance the rate of heating or cooling in the advanced technological processes through nanofluids. However, the effects of synchronized magnetic and electric fields on mixed convection are deliberated. Viscous dissipation and thermal radiation are considered on the energy field, as well as Ohmic heating. The existence of chemical reaction on the nanoparticle concentration field performed. No study so far has been conducted in esteems to the problem mentioned featuring nanofluid flow against vertical stretching. Consequently, this study targets to bridge the gap and also gives the idea to be the first attempt in this respect. Numerical solutions are achieved using implicit finite difference scheme known as Keller box method [40,41]. The impacts of incipient parameters from the fields are presented and discussed. The skin friction coefficient, local Nusselt and Sherwood numbers are deliberate numerically and reflected accordingly.

2. Mathematical formulation

Consider the unsteady mixed convective flow of an electrically-conducting nanofluid over a stretching sheet subjected to slips and double stratification. The coordinate system is Cartesian chosen, x-lengthwise the stretching-material and y-lengthwise designates the perpendicular position at the material surface. (u, v) symbolizes the velocity constituents directly towards $x-$ connecting to y-direction (see Fig. 1). The fluid-velocity indicated as $u_W(x,t) = bx/(1-at)$, where (a,b) are constants coefficient of the stretching with dimension $(\text{time})^{-1}$ for $(at < 1, a \geq 0)$. Applied magnetic and electric fields upon intensities performances alongside the defined direction. Magnetic-field including electric field adheres to Ohm's law outline $\bar{J} = \sigma\left(\bar{E} + \bar{V} \times \bar{B}\right)$ [42] whereby $\bar{J}, \sigma, \bar{V}$ takes Joule-

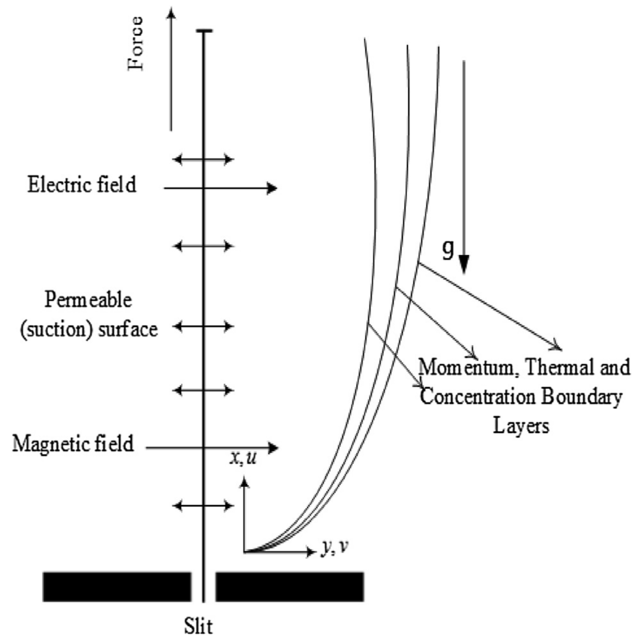

Fig. 1 Geometrical sketch.

current, electrical conductivity, besides the velocity of the fluid. Magnetic field as well as the electric field of strengths symbolize by $\bar{B}(t) = B_0/\sqrt{1-at}$ and $\bar{E}(t) = E_0/\sqrt{1-at}$ are functional normal on the sheet, the Reynolds magnetic number is considered insignificant [43]. The induced magnetic field and Hall current effects are ignored subject to small magnetic Reynolds number. Heat transport is inspected subject toward radiative transfer, viscous-dissipation, and Ohmic heating. Using Rosseland and boundary layer approximations, resulted in,

$$\frac{\partial u}{\partial x} + \frac{\partial v}{\partial y} = 0, \tag{1}$$

$$\frac{\partial u}{\partial t} + u\frac{\partial u}{\partial x} + v\frac{\partial u}{\partial y} = \nu\left(\frac{\partial^2 u}{\partial y^2}\right) + \frac{\sigma(EB - B^2 u)}{\rho_f} + \frac{g\left[(1-\varphi_\infty)\rho_{f\infty}\beta_T(T-T_\infty) - (\rho_p - \rho_{f\infty})\beta_\varphi(\varphi-\varphi_\infty)\right]}{\rho_f}, \tag{2}$$

$$\frac{\partial T}{\partial t} + u\frac{\partial T}{\partial x} + v\frac{\partial T}{\partial y} = \frac{k}{(\rho c)_f}\left(\frac{\partial^2 T}{\partial y^2}\right) + \frac{1}{(\rho c)_f}\left(\frac{16T_\infty^3\sigma^*}{3k^*}\frac{\partial^2 T}{\partial y^2}\right) + \frac{\mu}{(\rho c)_f}\left(\frac{\partial u}{\partial y}\right)^2 + \tau\left\{D_B\left(\frac{\partial \varphi}{\partial y}\frac{\partial T}{\partial y}\right) + \frac{D_T}{T_\infty}\left(\frac{\partial T}{\partial y}\right)^2\right\}, \tag{3}$$

$$\frac{\partial \varphi}{\partial t} + u\frac{\partial \varphi}{\partial x} + v\frac{\partial \varphi}{\partial y} = D_B\left(\frac{\partial^2 \varphi}{\partial y^2}\right) + \frac{D_T}{T_\infty}\left(\frac{\partial^2 T}{\partial y^2}\right) - k_1(\varphi - \varphi_\infty). \tag{4}$$

The boundary conditions

$$y = 0: \quad u = u_w(x,t) + l_1\frac{\partial u}{\partial y}, \quad v = v_w(x,t),$$

$$T = T_W(x,t) + l_2\frac{\partial T}{\partial y}, \quad \varphi = \varphi_W(x,t) + l_3\frac{\partial \varphi}{\partial y}, \tag{5}$$

$$y \to \infty: \quad u \to 0, \quad T \to T_\infty, \quad \varphi \to \varphi_\infty \tag{6}$$

where

$$u_W(x,t) = bx/(1-at), \quad T_W(x,t) = T_0 + A_1x(1-at)^{-1},$$

$$\varphi_W(x,t) = \varphi_0 + C_1x(1-at)^{-1}, \quad T_\infty = T_0 + A_2x(1-at)^{-1},$$
$$\varphi_\infty = \varphi_0 + C_2x(1-at)^{-1}.$$

Here $l_1 = l_1'\sqrt{1-at}, l_2 = l_2'\sqrt{1-at}, l_3 = l_3'\sqrt{1-at}$, which represents the velocity slip factor, temperature slip factor, concentration slip factor [44,45]. A_1, A_2, C_1, and C_2 are the dimensional constants for thermal and solutal stratifications factors. However, $v_w = -v_0/\sqrt{1-at}$ denote the mass-transfer at the wall, and $v_w < 0$ as flow due to injection whereas $v_w > 0$ depicts the suction-flow. The notation $\alpha = k/(\rho c)_f, g, \mu, \rho_f, \rho_p, D_B, D_T, k_1 = k_0/(1-at)$and $\tau = (\rho c)_p/(\rho c)_f$ are the fluid thermal diffusivity, gravitational acceleration, fluid kinematic viscosity, fluid density, density with respect to particles, Brownian diffusion coefficient, the thermophoresis diffusion coefficient, the rate of chemical reaction, and the nanoparticles material heat transfer capacity to the fluid heat capacity respectively.

The system of Eqs. (1)–(6) can be reduced by using the similarities variables defined as:

$$\psi = \sqrt{\frac{bv}{1-at}}xf(\eta), \quad \eta = y\sqrt{\frac{b}{v(1-at)}}, \quad \theta = \frac{T-T_\infty}{T_w - T_0},$$
$$\phi = \frac{\varphi - \varphi_\infty}{\varphi_w - \varphi_0}, \tag{7}$$

The stream function ψ can be expressed as:

$$u = \frac{\partial \psi}{\partial y}, \quad v = -\frac{\partial \psi}{\partial x} \tag{8}$$

Using Eqs. (7) and (8) into Eqs. (1)–(6), the velocity, temperature and nanoparticles concentration with boundary conditions are presented as follow,

$$f_{\eta\eta\eta} + ff_{\eta\eta} - f_\eta^{\,2} - \delta\left(f_\eta + \frac{\eta}{2}f_{\eta\eta}\right) + M\left(E_1 - f_\eta\right) + \lambda(\theta - N\phi) = 0, \tag{9}$$

$$\frac{1}{Pr}\left(1 + \frac{4}{3}Rd\right)\theta_{\eta\eta} + f\theta_\eta - f_\eta\theta - \delta\left(s_t + \frac{\eta}{2}\theta_\eta + \theta\right) + Nb\phi_\eta\theta_\eta$$
$$+ Nt\theta_\eta^{\,2} + Ec\left(f_{\eta\eta}\right)^2 + MEc\left(f_\eta - E_1\right)^2 - s_tf_\eta = 0, \tag{10}$$

$$\phi_{\eta\eta} + Scf\phi_\eta - Scf_\eta\phi - Sc\delta\left(s_m + \frac{\eta}{2}\phi_\eta + \phi\right)$$
$$+ \frac{Nt}{Nb}\theta_{\eta\eta} - Sc\gamma\phi - Scs_mf_\eta = 0, \tag{11}$$

Boundary conditions:

$$f = s, \quad f_\eta = 1 + L_1f_{\eta\eta}, \quad \theta = 1 - s_t + L_2\theta_\eta, \quad \phi$$
$$= 1 - s_m + L_3\phi_\eta, \quad \text{at} \quad \eta = 0 \tag{12}$$

$$f_\eta = 0, \quad \theta = 0, \quad \phi = 0, \quad \text{as} \quad \eta \to \infty. \tag{13}$$

The dimensionless nanoparticle concentration is connected withϕ, dimensionless temperature is associated with θ, dimensionless velocity is denoted as f_η. Also, $\lambda = Gr/Re^2$ is Richardson number known as mixed convection parameter: for the values of $(\lambda > 0)$accounts for heated surface, $(\lambda < 0)$ corresponds to cold surface, and $(\lambda = 0)$ indicates the forced convection flow. Again, we have the

Grashof parameter: $Gr = g\beta(1-\varphi_\infty)(T_W - T_0)\rho_{f\infty}/v^2\rho_f$,
Reynolds parameter: $Re = u_wx/v$,
Buoyancy ratio parameter: $N = (\rho_f - \rho_{f\infty})(\varphi_W - \varphi_0)/\beta\rho_{f\infty}(1-\varphi_\infty)(T_W - T_0)$,
Unsteadiness parameter: $\delta = a/b$,
Velocity slip parameter: $L_1 = l_1'\sqrt{b/v}$,
Thermal slip parameter: $L_2 = l_2'\sqrt{b/v}$,
Solutal slip parameter: $L_3 = l_3'\sqrt{b/v}$,
Thermal stratification parameter: $s_t = A_2/A_1$,
Concentration stratification parameter: $s_m = C_2/C_1$,
Prandtl number: $= v/\alpha$,
Brownian motion parameter: $Nb = (\rho c)_pD_B(\varphi_w - \varphi_0)/(\rho c)_fv$,
Thermophoresis number:$Nt = (\rho c)_pD_T(T_w - T_0)/(\rho c)_fvT_\infty$,
Schmidt number: $Sc = v/D_B$,
Magnetic field parameter: $M = \sigma B_0^2/b\rho_f$,
Electric field parameter: $E_1 = E_0/u_WB_0$,
Eckert number: $Ec = u_W^2/c_p(T_w - T_0)$,
Radiation parameter: $Rd = 4\sigma^*T_\infty^3/k^*k$,

Parameter viz chemical reaction $\gamma = k_0/b$ inasmuch that $(\gamma > 0)$ allied to destructive-chemical-reaction flow and $(\gamma < 0)$ connected to the generative-chemical-reaction parameter.

Parameter viz $s = v_0/\sqrt{vb}$ denote suction $(s > 0)$ whereas $(s < 0)$ associated with injection respectively.

Now, the defined local Sherwood number, the local Nusselt number and then skin friction coefficient, are given as:

$$Sh = \frac{xq_m}{D_B(\varphi_w - \varphi_0)}, \quad Nu = \frac{xq_w}{k(T_w - T_0)}, \quad c_f = \frac{\tau_w}{\rho u_w^2(x,t)}, \tag{14}$$

here

$$q_m = -D_B\left(\frac{\partial \varphi}{\partial y}\right)_{y=0}, q_w = -\left(\left(k + \frac{16\sigma^*T_\infty^3}{3k^*}\right)\frac{\partial T}{\partial y}\right)_{y=0}, \tau_w = \mu_f\left(\frac{\partial u}{\partial y}\right)_{y=0}, \tag{15}$$

τ_w represents the shear stress of the nanofluid,
q_w associates with surface heat flux,
q_m accounts for surface mass flux, and then
k is linked to nanofluid thermal conductivity.

In non-dimensional form, the local skin-friction-coefficient, local Nusselt and Sherwood numbers are expressed as:

$$Re^{\frac{1}{2}}c_f = f_{\eta\eta}(0), \quad Nu/Re^{\frac{1}{2}} = -\left(1 + \tfrac{4}{3}Rd\right)\left(\tfrac{1}{1-s_t}\right)\theta_\eta(0),$$
$$Sh/Re^{\frac{1}{2}} = -\left(\tfrac{1}{1-s_m}\right)\phi_\eta(0). \tag{16}$$

3. Results and discussion

In this investigation, the unsteady mixed convection for electromagnetic flow of nanofluid over stretchable sheet is deliberated with double stratification and slip conditions. The governing Eqs. (9)–(11) subjected to the boundary conditions (12) and (13) were solved numerically. Results validation, are compared with the previous published work of [46], see Table 1 and velocity profile in Fig. 2. The based fluid value for Prandtl number is fixed $Pr = 6.2$ (that is water), and the selection of values for other parameters follows [18,19,29,34–37] in the computation. According to these results using the Keller box method see [47–50], shows good agreement in limiting sense.

Velocity profiles $f_\eta(\eta)$: Fig. 3 portrays the variation of magnetic field M on the velocity profile $f_\eta(\eta)$ along the stretching sheet. Both velocity and momentum boundary layer thickness are reduced for larger values of magnetic field parameter. Physically with an increase in magnetic field parameter, the Lorentz force increases and hence the velocity of nanofluid decreases. Lorentz forces drag the magnetic nanoparticles as results of that, the strength of the velocity reduced, for an enhancement of the magnetic field. Fig. 4, shows the variation on the velocity field $f_\eta(\eta)$with respect to electric field E_1. Involvement of electric field applied normal, it encourages nanofluid acceleration adjacent the stretchable surface. Consequently, the velocity and momentum boundary layer thickness intensifies for augmentation. As a result, the flow in uphill-way heightens as the accelerating force attributed to the Lorentz force reinforces. Fig. 5 depicts the velocity profile $f_\eta(\eta)$ for nanofluid flow over a linear stretching sheet decreased with

Table 1 Assessment of the skin friction coefficient $-f_{\eta\eta}(0)$ when $N = \lambda = 0$.

M	s	E_1	δ	Present results	Ref. [46]
0	0.5	0.0	0.0	1.280777	1.2808
0.5				1.500000	1.5000
1.0				1.686141	1.6861
1.5				1.850781	1.8508
2.0				2.000000	2.0000
1.0	0			1.414214	1.4142
	0.2			1.517745	1.5177
	0.7			1.806880	1.8069
	1.0			2.000000	2.0000
	0.2	0.1		1.335083	
		0.3		1.003660	
		0.5		0.698797	
		0.1	0.2	1.400699	
			0.7	1.547543	
			1.5	1.774626	

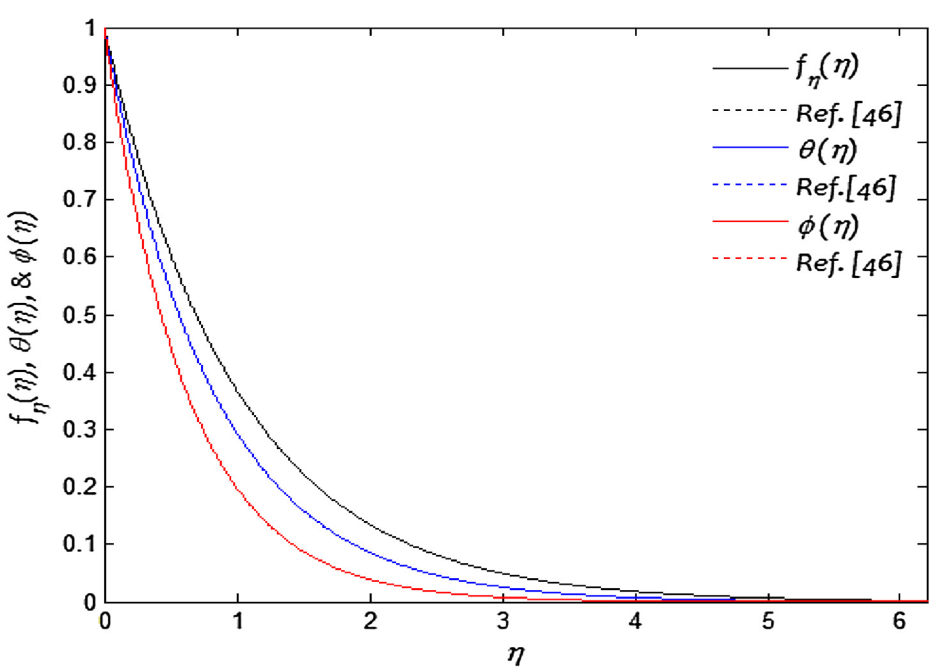

Fig. 2 Comparison of the results with the previously published studies of Ref. [46] for $f_\eta(\eta), \theta(\eta) \& \phi(\eta)$ when $N = \lambda = E_1 = \delta = 0$.

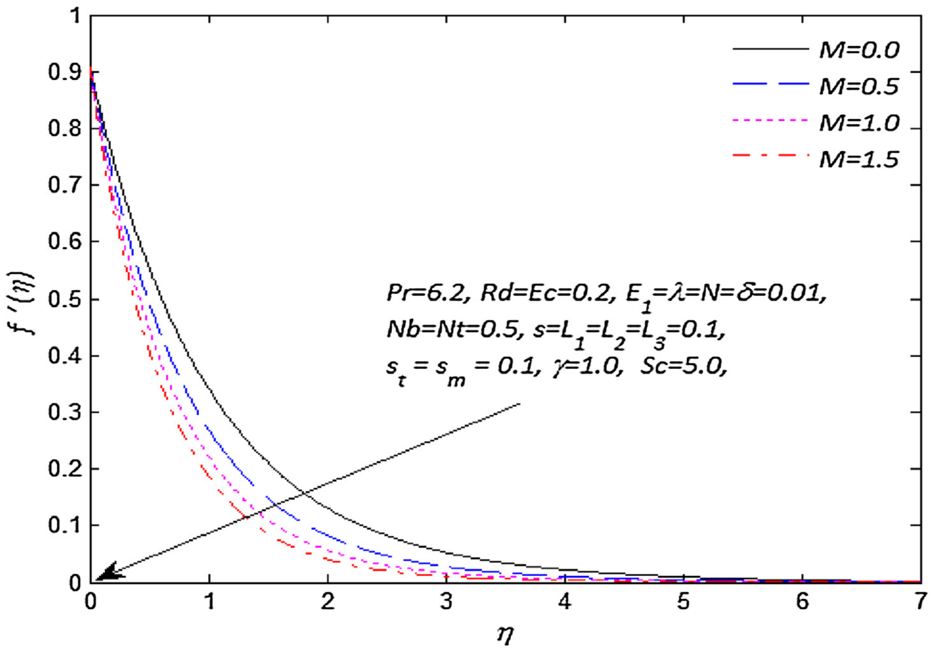

Fig. 3 Variation regarding M over velocity field.

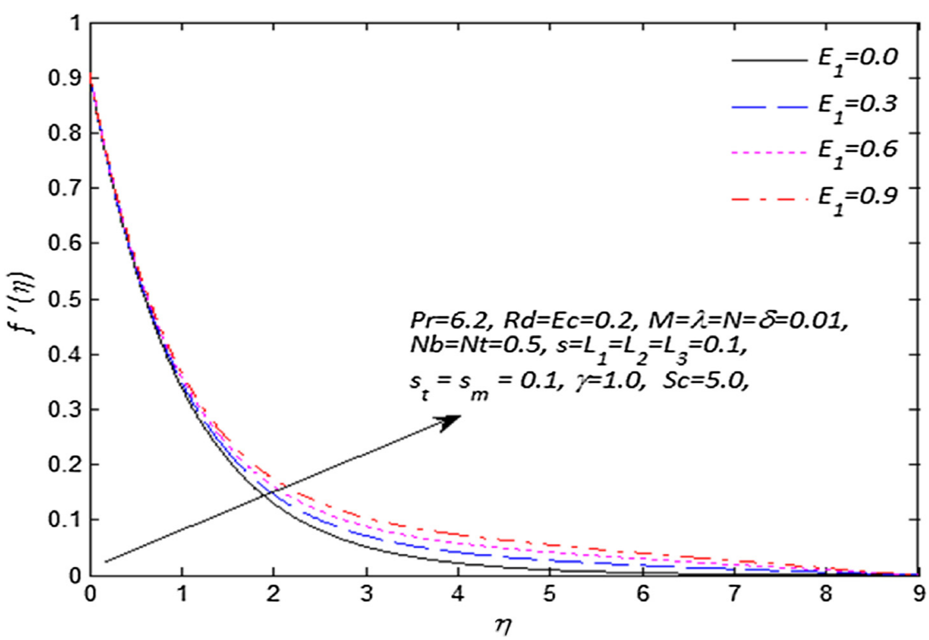

Fig. 4 Variation regarding E_1 over velocity field.

an intense amount of velocity slip parameter L_1. The influence of momentum slip create the velocity of nanofluid away from the sheet at initial stage and then the velocity of nanofluid flow steadily, which gives an insight on the occurrence of intersection close the sheet and declines asymptotically to zero near the stretching sheet of the momentum boundary layer. Consequently, the momentum boundary layer thickness for nanofluids reduces as the slip parameter rises.

Temperature profiles $\theta(\eta)$: Fig. 6 demonstrates the behavior of thermal radiation parameter Rd on temperature profile $\theta(\eta)$ over the stretching sheet. Intensification in thermal radiation results in heightening of nanofluid temperature and thermal layer thickness over the sheet surface. Accumulative thermal radiation involvement divulges that the absorption coefficient decayed gradually as the nanofluid flow over the stretching sheet. Thus, enhancement of the temperature profile. Fig. 7 depicts the variation in temperature profile with the impact of thermal stratification parameter s_t. It was noticed that the temperature and thermal layer thickness substantially drops as the thermal stratification accumulates. Also, this designates

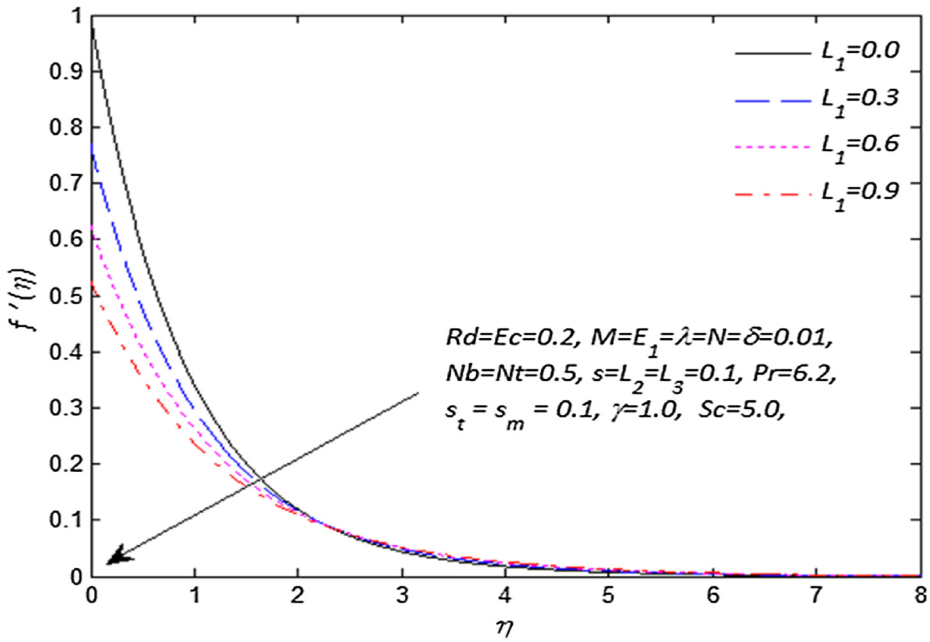

Fig. 5 Variation regarding L_1 over velocity field.

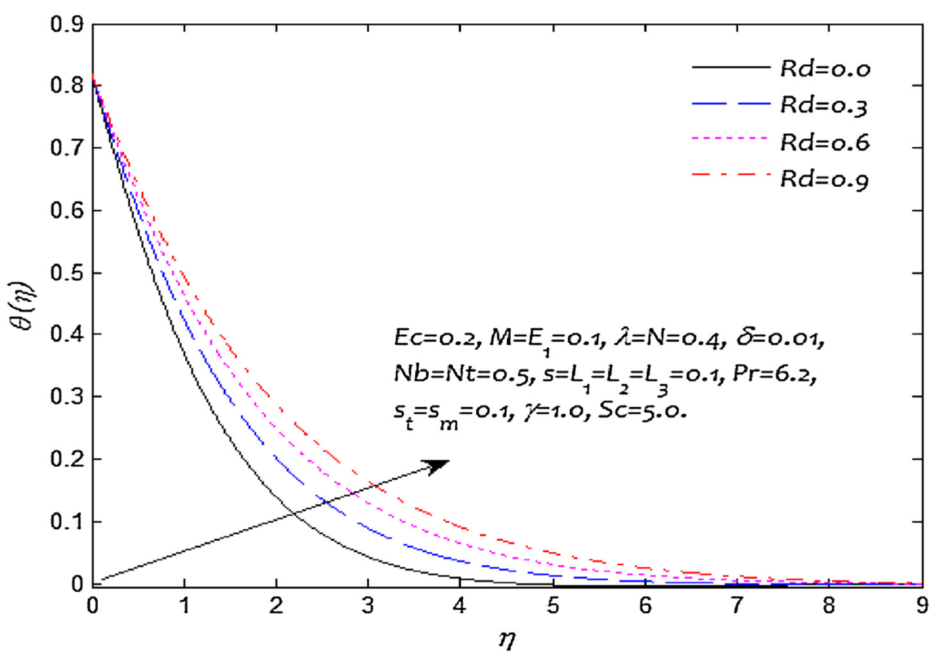

Fig. 6 Variation regarding Rd over temperature field.

an increase in free stream temperature or reduction in nanofluid surface temperature. The existence of thermal stratification influences the temperature of the nanofluid such that, it raises the ambient temperature or results to decay in surface temperature. This behavior frequently happens when heat is moving from hotter region to a colder region. The field steadily reduced as results of temperature difference which gradually declining between ambient fluid and surface of the sheet. Fig. 8 confirms the variation of temperature field $\theta(\eta)$ with respect to thermal slip parameter L_2. It was revealed that the temperature of the nanofluid and thermal layer thickness declined when the values of thermal slip parameter intensified.

Concentration profiles $\phi(\eta)$: The variation of concentration stratification parameter s_m on the concentration field is exhibited in Fig. 9. It is scrutinized that the volumetric fraction tight to the surface and the reference nanoparticles decayed when concentration stratification enhances. Therefore the concentration profile decayed over the stretching sheet. Note that, an increase in concentration stratification parameter results in a decrease in the concentration difference between the ambient

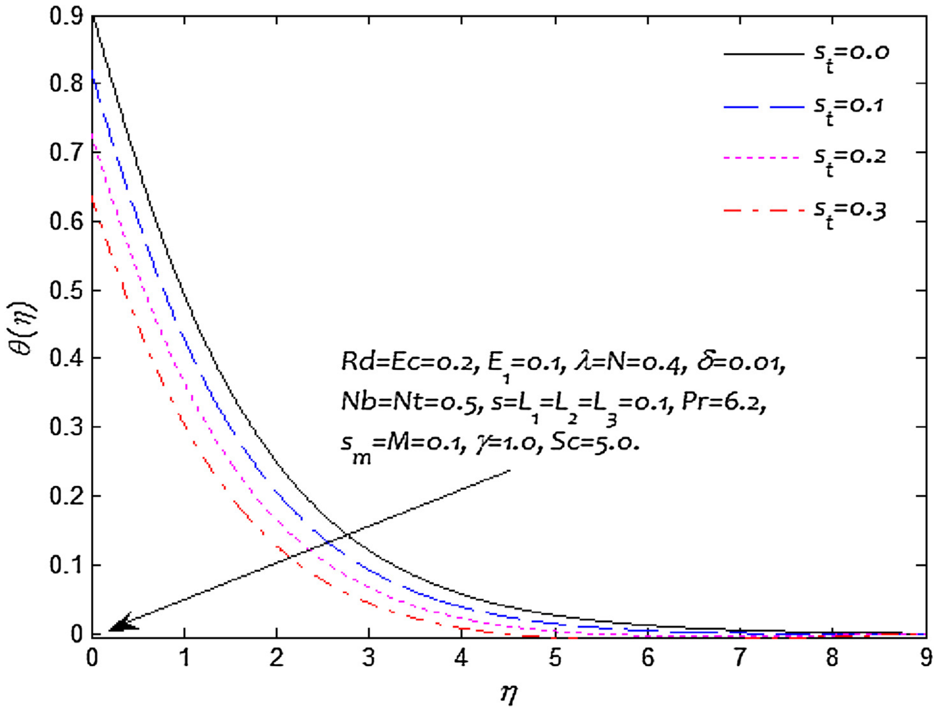

Fig. 7 Variation regarding s_t over temperature field.

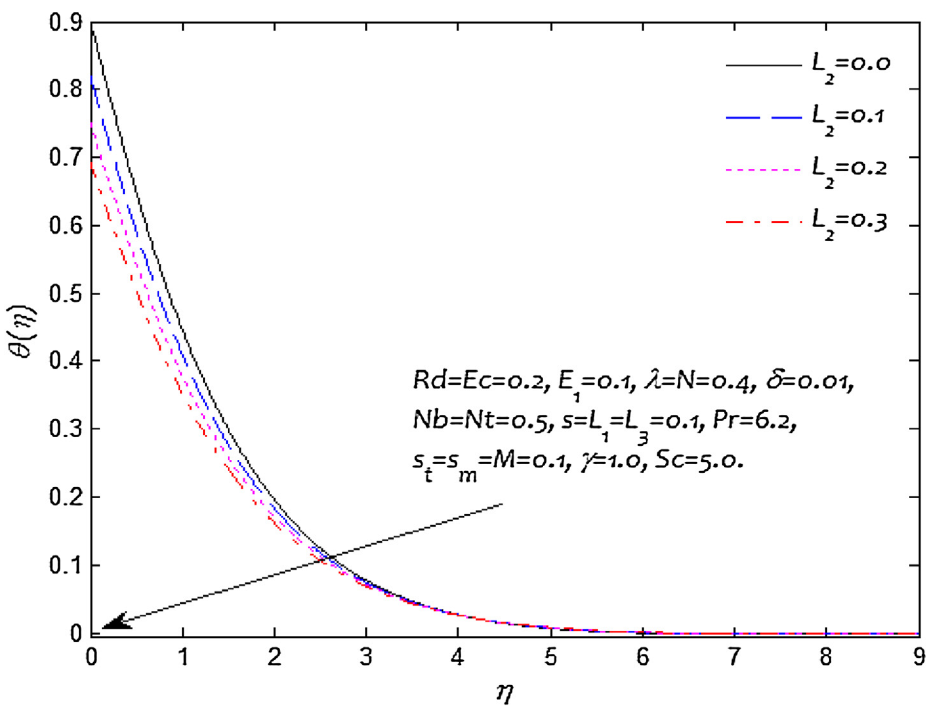

Fig. 8 Variation regarding L_2 over temperature field.

fluid and the linear stretching sheet. Fig. 10 proves the difference of nanoparticles concentration due to solutal slip parameter L_3. As it worth noticed from the graph, enhancement in solutal slip parameter decreases amount of nanoparticles fluid-concentration distance away from the wall and its related concentration layer thickness.

The skin friction coefficient with cumulative parameters for electric field, velocity slip, and mixed convection, as demonstrated in Fig. 11. The skin friction decreased due to an increase in accelerating body force from the fluid particles applied to the sheet to the nanofluid directly above the sheet surface. At a higher rate of the electric field, the skin friction

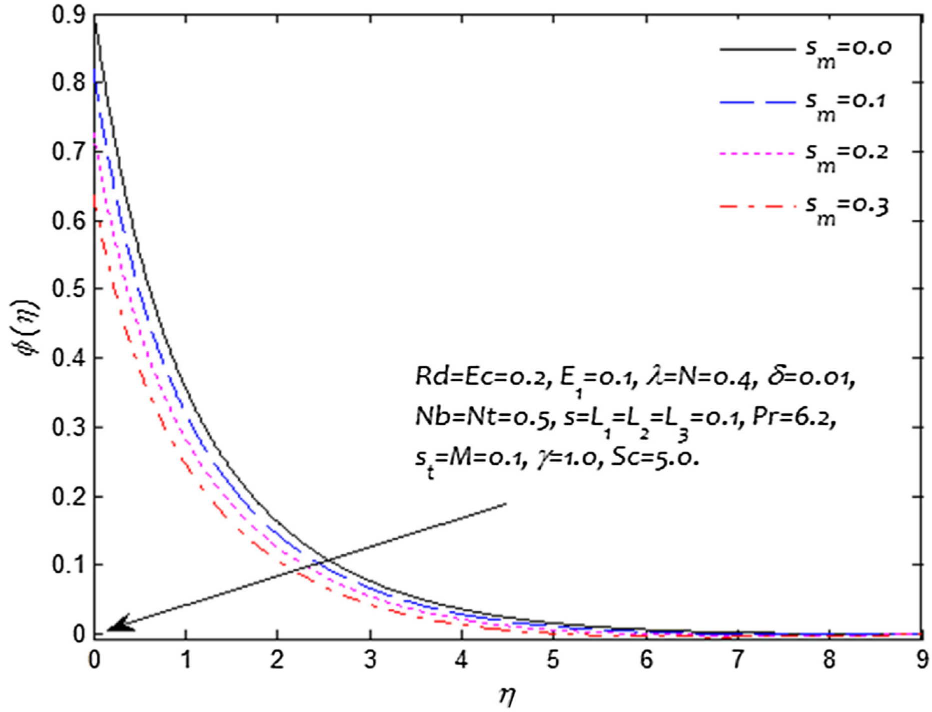

Fig. 9 Variation regarding s_m over the concentration field.

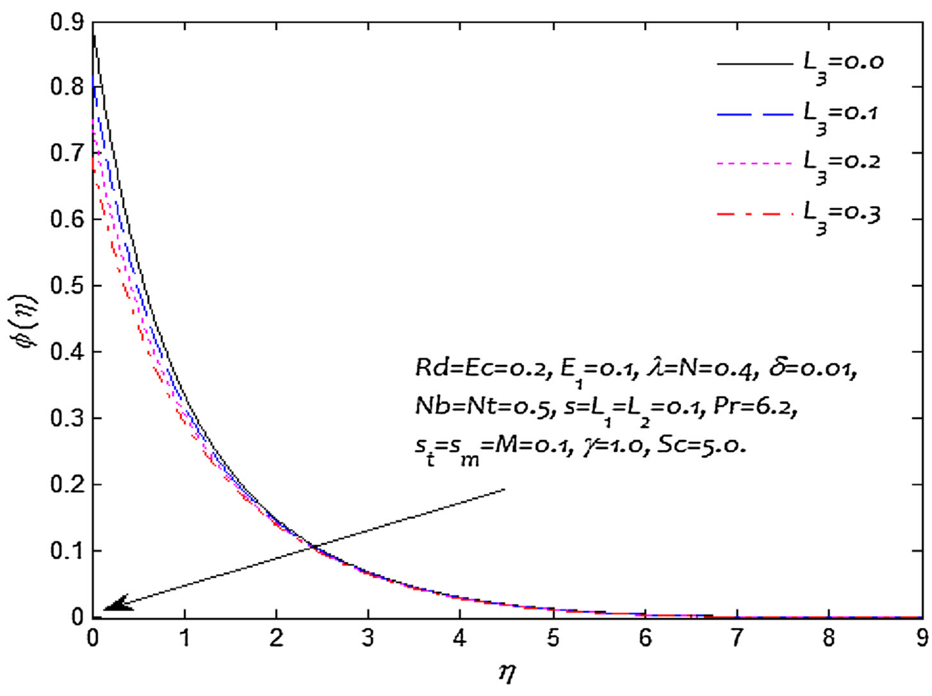

Fig. 10 Variation regarding L_3 over concentration field.

is found to be lower and increases with a decrease in the electric field. The mixed convection and velocity slip parameters decreased the frictional drag forces of the nanofluid over the stretching sheet surface for higher values.

Fig. 12 proves the impacts of thermal stratification, magnetic field and Brownian motion parameters on the dimensionless heat transfer rate at the sheet surface. It can be perceived that the reduced Nusselt number reduces with increasing Brownian motion, thermal stratification, and magnetic field. The Nusselt number is the ratio of convective to conductive heat transfer at a boundary in a nanofluid. So, the main attributes connecting with the thermal energy of nanofluid increases with Brownian motion and magnetic field within the thermal boundary layer. The convection includes both advection and diffusion. Thus, this invariably leads to weaken the rate of heat transfer over the sheet surface of the nanofluid.

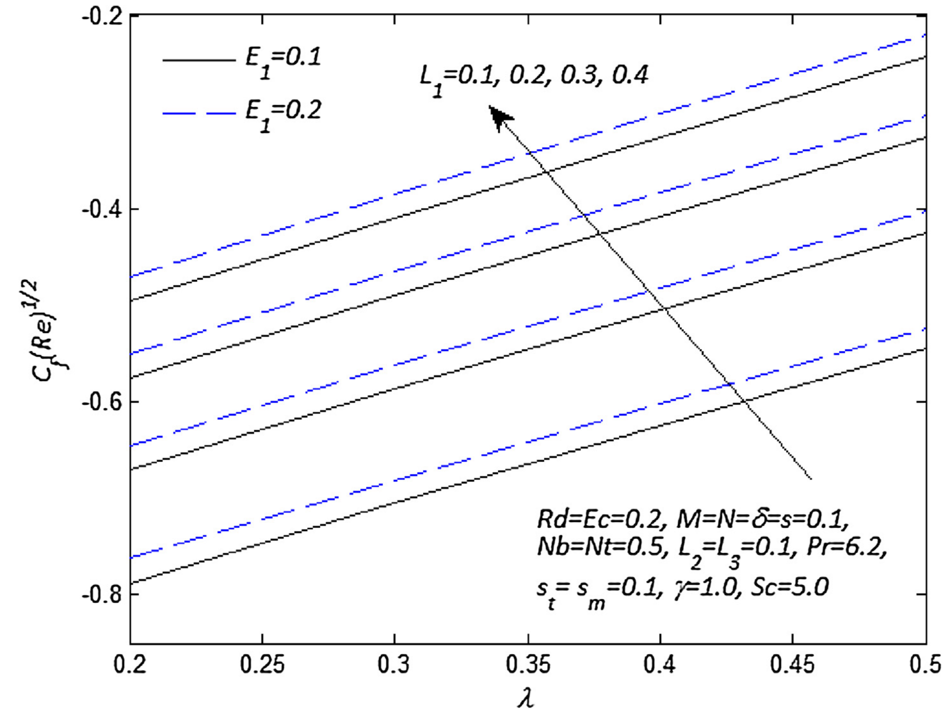

Fig. 11 Variations regarding E_1 and λ over skin friction coefficient.

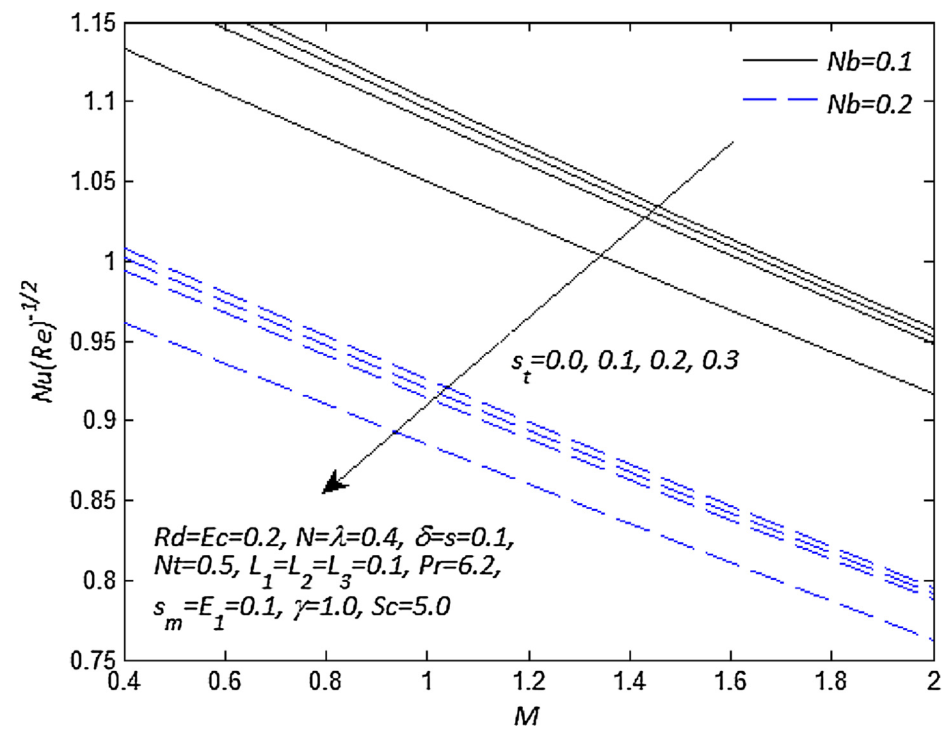

Fig. 12 Variations regarding s_t and M over Nusselt number.

It is also noticed that the Nusselt numbers are higher for smaller values of thermal stratification. The conductive component is measured under the same conditions as the convective nevertheless for the working nanofluid.

The influences of parameters distinction on reduced Sherwood numbers are depicted in Fig. 13. It is worth noticing that, the mass transfer rate of the nanoparticle concentration intensifies with increasing Schmidt number. Whereas the mass stratification uniquely decreased with the destructive chemical reaction when $\gamma = 1.0$ (i.e. the rate of diffusive mass transport increased) and increased when $\gamma = 0.1$ (i.e. the convective mass transfer increased). This unveils the fact that chemical reaction

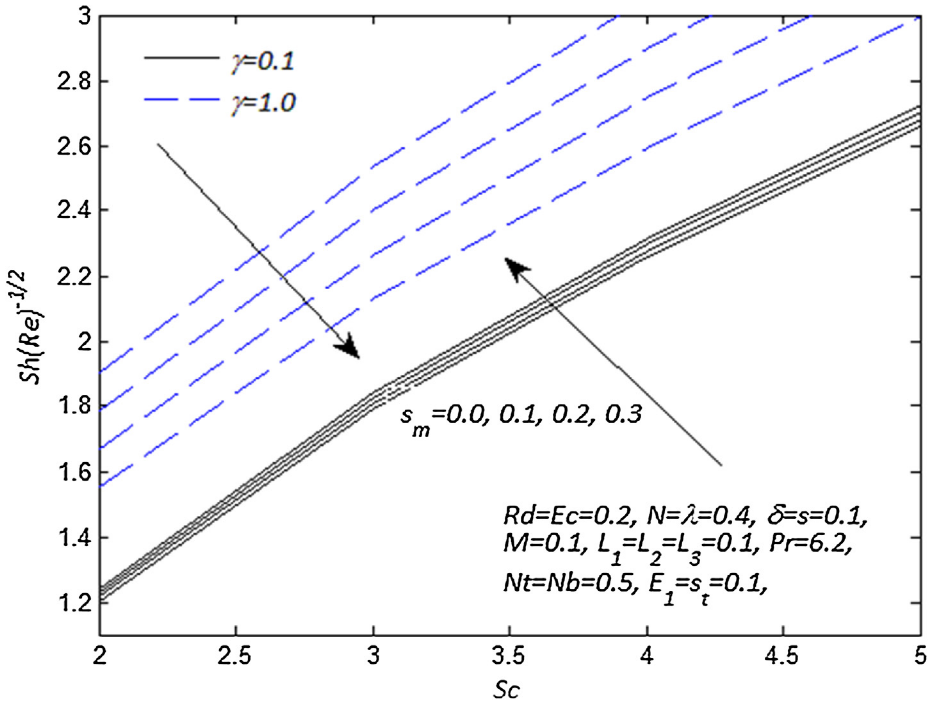

Fig. 13 Variations regarding s_m and Sc over Sherwood number.

decreased the nanoparticles concentration leading to rising in the mass transport rate noticed over the surface.

4. Concluding remark

The unsteady EMHD mixed convection flow of nanofluid over a stretching sheet is simulated using implicit finite difference known Keller box. In order to simulate nanofluid flow in vertical permeable stretching sheet, the Buongiorno mathematical model is used. Simultaneously the slips and double stratification were considered. The governing equation, the effects of both electric and magnetic fields function are used. The following momentous results are drawn from this investigation:

1. Nanofluid velocity advances along intensification involving electric field, nonetheless with lessening magnetic field and velocity slip parameters.
2. Nanofluid thermal energy intensifies with a rise in radiative transfer however, it decayed with thermal slip and thermal stratification parameters.
3. Nanoparticles concentration diminished with solutal slip and concentration of stratification parameters.
4. Skin friction coefficient reduces from increasing in mixed convection and velocity slip parameters.
5. Reduced Nusselt and Sherwood numbers decayed with stratification parameters, but the destructive chemical reaction parameter intensified with Sherwood number.

Acknowledgments

The authors would like to acknowledge Ministry of Education (MOE) and Research Management Centre (RMC), UTM for the financial support through vote numbers (Q.J091000.23C9.01D01 and 03G96) for this research. Also, Yahaya Shagaiya Daniel thankfully acknowledges financial support from TETFUND through Kaduna State University, Nigeria.

Declaration of Competing Interest

No conflict of interest.

References

[1] S.U. Choi, J.A. Eastman, Enhancing Thermal Conductivity of Fluids with Nanoparticles, Argonne National Lab, IL (United States), 1995.
[2] M. Sheikholeslami, B. Rezaeianjouybari, M. Darzi, A. Shafee, Z. Li, T.K. Nguyen, Application of nano-refrigerant for boiling heat transfer enhancement employing an experimental study, Int. J. Heat Mass Transf. 141 (2019) 974–980.
[3] M. Sheikholeslami, M. Jafaryar, M. Hedayat, A. Shafee, Z. Li, T.K. Nguyen, M. Bakouri, Heat transfer and turbulent simulation of nanomaterial due to compound turbulator including irreversibility analysis, Int. J. Heat Mass Transf. 137 (2019) 1290–1300.
[4] M. Sheikholeslami, M. Jafaryar, A. Shafee, Z. Li, R.-U. Haq, Heat transfer of nanoparticles employing innovative turbulator considering entropy generation, Int. J. Heat Mass Transf. 136 (2019) 1233–1240.
[5] M. Sheikholeslami, R.-U. Haq, A. Shafee, Z. Li, Y.G. Elaraki, I. Tlili, Heat transfer simulation of heat storage unit with nanoparticles and fins through a heat exchanger, Int. J. Heat Mass Transf. 135 (2019) 470–478.
[6] M. Sheikholeslami, R.-U. Haq, A. Shafee, Z. Li, Heat transfer behavior of nanoparticle enhanced PCM solidification through an enclosure with V shaped fins, Int. J. Heat Mass Transf. 130 (2019) 1322–1342.

[7] M. Sheikholeslami, New computational approach for exergy and entropy analysis of nanofluid under the impact of Lorentz force through a porous media, Comput. Methods Appl. Mech. Eng. 344 (2019) 319–333.
[8] Y.S. Daniel, Z.A. Aziz, Z. Ismail, F. Salah, Entropy analysis of unsteady magnetohydrodynamic nanofluid over stretching sheet with electric field, Int. J. Multiscale Comput. Eng. 15 (6) (2017).
[9] M. Sheikholeslami, M. Jafaryar, J.A. Ali, S.M. Hamad, A. Divsalar, A. Shafee, T. Nguyen-Thoi, Z. Li, Simulation of turbulent flow of nanofluid due to existence of new effective turbulator involving entropy generation, J. Mol. Liq. 291 (2019) 111283.
[10] E. Magyari, A. Chamkha, Exact analytical results for the thermosolutal MHD Marangoni boundary layers, Int. J. Therm. Sci. 47 (7) (2008) 848–857.
[11] M. Modather, A. Chamkha, An analytical study of MHD heat and mass transfer oscillatory flow of a micropolar fluid over a vertical permeable plate in a porous medium, Turk. J. Eng. Environ. Sci. 33 (4) (2010) 245–258.
[12] A.J. Chamkha, Coupled heat and mass transfer by natural convection about a truncated cone in the presence of magnetic field and radiation effects, Numeric. Heat Transfer: Part A: Appl. 39 (5) (2001) 511–530.
[13] R.S.R. Gorla, A. Chamkha, Natural convective boundary layer flow over a nonisothermal vertical plate embedded in a porous medium saturated with a nanofluid, Nanoscale Microscale Thermophys. Eng. 15 (2) (2011) 81–94.
[14] A.J. Chamkha, S. Abbasbandy, A. Rashad, K. Vajravelu, Radiation effects on mixed convection about a cone embedded in a porous medium filled with a nanofluid, Meccanica 48 (2) (2013) 275–285.
[15] Y.S. Daniel, Z.A. Aziz, Z. Ismail, F. Salah, Entropy analysis in electrical magnetohydrodynamic (MHD) flow of nanofluid with effects of thermal radiation, viscous dissipation, and chemical reaction, Theor. Appl. Mech. Lett. 7 (4) (2017) 235–242.
[16] E. Magyari, A.J. Chamkha, Combined effect of heat generation or absorption and first-order chemical reaction on micropolar fluid flows over a uniformly stretched permeable surface: the full analytical solution, Int. J. Therm. Sci. 49 (9) (2010) 1821–1828.
[17] P.S. Reddy, P. Sreedevi, A.J. Chamkha, MHD boundary layer flow, heat and mass transfer analysis over a rotating disk through porous medium saturated by Cu-water and Ag-water nanofluid with chemical reaction, Powder Technol. 307 (2017) 46–55.
[18] Y.S. Daniel, Z.A. Aziz, Z. Ismail, A. Bahar, F. Salah, Slip role for unsteady MHD mixed convection of nanofluid over stretching sheet with thermal radiation and electric field, Indian J. Phys. (2019) 1–13.
[19] Y.S. Daniel, Z.A. Aziz, Z. Ismail, A. Bahar, F. Salah, Stratified electromagnetohydrodynamic flow of nanofluid supporting convective role, Korean J. Chem. Eng. 36 (7) (2019) 1021–1032.
[20] Y.S. Daniel, Steady MHD laminar flows and heat transfer adjacent to porous stretching sheets using HAM, Am. J. Heat Mass Transfer 2 (3) (2015) 146–159.
[21] A.J. Chamkha, R. Mohamed, S.E. Ahmed, Unsteady MHD natural convection from a heated vertical porous plate in a micropolar fluid with Joule heating, chemical reaction and radiation effects, Meccanica 46 (2) (2011) 399–411.
[22] A.J. Chamkha, A.-R.A. Khaled, Similarity solutions for hydromagnetic mixed convection heat and mass transfer for Hiemenz flow through porous media, Int. J. Numer. Meth. Heat Fluid Flow 10 (1) (2000) 94–115.
[23] P.S. Reddy, A.J. Chamkha, Soret and Dufour effects on MHD convective flow of Al2O3–water and TiO2–water nanofluids past a stretching sheet in porous media with heat generation/absorption, Adv. Powder Technol. 27 (4) (2016) 1207–1218.
[24] C. RamReddy, P. Murthy, A.J. Chamkha, A. Rashad, Soret effect on mixed convection flow in a nanofluid under convective boundary condition, Int. J. Heat Mass Transf. 64 (2013) 384–392.
[25] A. Chamkha, Solar radiation assisted natural convection in uniform porous medium supported by a vertical flat plate, 1997.
[26] A. Al-Mudhaf, A.J. Chamkha, Similarity solutions for MHD thermosolutal Marangoni convection over a flat surface in the presence of heat generation or absorption effects, Heat Mass Transf. 42 (2) (2005) 112–121.
[27] A.J. Chamkha, A.F. Al-Mudhaf, I. Pop, Effect of heat generation or absorption on thermophoretic free convection boundary layer from a vertical flat plate embedded in a porous medium, Int. Commun. Heat Mass Transfer 33 (9) (2006) 1096–1102.
[28] Y.S. Daniel, S.K. Daniel, Effects of buoyancy and thermal radiation on MHD flow over a stretching porous sheet using homotopy analysis method, Alexandria Eng. J. 54 (3) (2015) 705–712.
[29] T. Hayat, A. Nassem, M.I. Khan, M. Farooq, A. Al-Saedi, Magnetohydrodynamic (MHD) flow of nanofluid with double stratification and slip conditions, Phys. Chem. Liq. 56 (2) (2018) 189–208.
[30] A.J. Chamkha, Hydromagnetic natural convection from an isothermal inclined surface adjacent to a thermally stratified porous medium, Int. J. Eng. Sci. 35 (10–11) (1997) 975–986.
[31] Y.S. Daniel, Z.A. Aziz, Z. Ismail, F. Salah, Effects of thermal radiation, viscous and Joule heating on electrical MHD nanofluid with double stratification, Chin. J. Phys. 55 (3) (2017) 630–651.
[32] R. Kandasamy, R. Dharmalingam, K.S. Prabhu, Thermal and solutal stratification on MHD nanofluid flow over a porous vertical plate, Alexandria Eng. J. 57 (1) (2018) 121–130.
[33] A.J. Chamkha, MHD-free convection from a vertical plate embedded in a thermally stratified porous medium with Hall effects, Appl. Math. Model. 21 (10) (1997) 603–609.
[34] Y.S. Daniel, Z.A. Aziz, Z. Ismail, F. Salah, Double stratification effects on unsteady electrical MHD mixed convection flow of nanofluid with viscous dissipation and Joule heating, J. Appl. Res. Technol. 15 (5) (2017) 464–476.
[35] T. Hayat, F. Shah, Z. Hussain, A. Alsaedi, Outcomes of double stratification in Darcy-Forchheimer MHD flow of viscoelastic nanofluid, J. Braz. Soc. Mech. Sci. Eng. 40 (3) (2018) 145.
[36] T. Hayat, I. Ullah, A. Alsaedi, B. Ahmad, Variable aspects of double stratified MHD flow of second grade nanoliquid with heat generation/absorption: a revised model, Radiat. Phys. Chem. 157 (2019) 109–115.
[37] M. Waqas, A. Dogonchi, S. Shehzad, M.I. Khan, T. Hayat, A. Alsaedi, Nonlinear convection and joule heating impacts in magneto-thixotropic nanofluid stratified flow by convectively heated variable thicked surface, J. Mol. Liquids (2019) 111945.
[38] K.U. Rehman, M. Malik, Q.M. Al-Mdallal, M. Zahri, On both magnetized and non-magnetized dual stratified medium via stream lines topologies: a generalized formulation, Sci. Rep. 9 (2019).
[39] J. Buongiorno, Convective transport in nanofluids, J. Heat Transfer 128 (3) (2006) 240–250.
[40] A.J. Chamkha, A.-R.A. Khaled, Hydromagnetic combined heat and mass transfer by natural convection from a permeable surface embedded in a fluid-saturated porous medium, Int. J. Numer. Meth. Heat Fluid Flow 10 (5) (2000) 455–477.
[41] A.J. Chamkha, C. Issa, K. Khanafer, Natural convection from an inclined plate embedded in a variable porosity porous medium due to solar radiation, Int. J. Therm. Sci. 41 (1) (2002) 73–81.
[42] T. Hayat, A. Shafiq, A. Alsaedi, Effect of Joule heating and thermal radiation in flow of third grade fluid over radiative surface, Plos One 9 (1) (2014) e83153.
[43] K. Bhattacharyya, S. Mukhopadhyay, G. Layek, Unsteady MHD boundary layer flow with diffusion and first-order

chemical reaction over a permeable stretching sheet with suction or blowing, Chem. Eng. Commun. 200 (3) (2013) 379–397.

[44] Y.S. Daniel, Z.A. Aziz, Z. Ismail, F. Salah, Slip effects on electrical unsteady MHD natural convection flow of nanofluid over a permeable shrinking sheet with thermal radiation, Eng. Lett. 26 (1) (2018).

[45] Y.S. Daniel, Laminar convective boundary layer slip flow over a flat plate using homotopy analysis method, J. Inst. Eng. (India): Ser. E 97 (2) (2016) 115–121.

[46] W. Ibrahim, B. Shankar, MHD boundary layer flow and heat transfer of a nanofluid past a permeable stretching sheet with velocity, thermal and solutal slip boundary conditions, Comput. Fluids 75 (2013) 1–10.

[47] H. Takhar, A. Chamkha, G. Nath, Unsteady flow and heat transfer on a semi-infinite flat plate with an aligned magnetic field, Int. J. Eng. Sci. 37 (13) (1999) 1723–1736.

[48] T. Cebeci, P. Bradshaw, Physical and Computational Aspects of Convective Heat Transfer, Springer Science & Business Media, 1988.

[49] A. Chamkha, MHD flow of a micropolar fluid past a stretched permeable surface with heat generation or absorption, 2009.

[50] H.S. Takhar, A.J. Chamkha, G. Nath, MHD flow over a moving plate in a rotating fluid with magnetic field, Hall currents and free stream velocity, Int. J. Eng. Sci. 40 (13) (2002) 1511–1527.